Energetics of Third-Row Transition Metal Methylidene Ions MCH_2^+ (M = La, Hf, Ta, W, Re, Os, Ir, Pt, Au)

Karl K. Irikura† and William A. Goddard III*

Contribution from the Materials and Molecular Simulation Center, Beckman Institute (139-74), Division of Chemistry and Chemical Engineering,‡ California Institute of Technology, Pasadena, California 91125

Received February 28, 1994®

Abstract: High-level *ab initio* calculations, involving multireference configuration interaction and moderately large basis sets, have been performed to determine the metal–carbon bond energies in the metal methylidene ions MCH_2^+ of the 5d transition series. On the basis of our calculations and available experimental data, the recommended bond energies $D(M^+–CH_2)$ are 98 ± 1.5 (La), 104 ± 5 (Hf), 115 ± 5 (Ta), 111 ± 3 (W), 97 ± 4 (Re), 113 ± 3 (Os), 123 ± 5 (Ir), 123 ± 5 (Pt), and 94 ± 2 (Au) kcal/mol. These bond energies are consistent with the experimentally observed reactivity of the metal ions M^+ with methane. The double-humped pattern is explained in the context of promotion and exchange energies. The arguments are extended in order to estimate metal–methylidyne bond strengths $D(M^+–CH)$.

1. Introduction

It is known from both experiment[1] and theory[2] that third-row (5d) transition metals form much stronger bonds than do first-row (3d) and second-row (4d) transition metals. Indeed, recent gas-phase studies of the reactions of bare, third-row transition metal ions have revealed that methane is dehydrogenated spontaneously at room temperature by Ta^+, W^+, Os^+, Ir^+, and Pt^+ (reaction 1).[3–6] In contrast, reaction 1 is endothermic for all

$$M^+ + CH_4 \rightarrow MCH_2^+ + H_2 \qquad (1)$$

first- and second-row metals studied (with the possible exception[7,8] of Zr^+). For Ta^+ and W^+, sequential reactions with methane lead rapidly to the corresponding metallacyclopentane cations.[3–5] Although the reaction rates have been measured, a precise bond energy is available only for $LaCH_2^+$.[9] The present calculations were undertaken in order to determine the trends in bond strengths in third-row transition metal methylidene ions and to permit comparison of the kinetics and thermodynamics of reaction 1.

Two important resonance structures can be written to describe the bonding between a transition metal and a CH_2 moiety, as indicated in Scheme 1. At the covalent extreme, the σ bond involves one electron on the metal in an s + d_{z^2} hybrid orbital and one electron on the carbon in an sp^2-type orbital. Likewise, the

Scheme 1

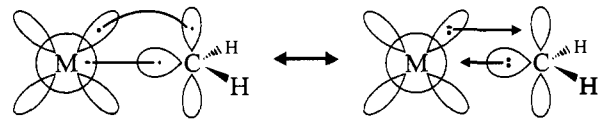

covalent (methylidene) dative (carbene)

π bond involves a metal d_{xz} orbital spin-paired with a carbon p_x orbital. This corresponds to a triplet methylene ($\sigma^1\pi^1$). Covalently bonded metal–methylene complexes of this type, such as $Cp_2Ta(CH_3)(CH_2)$, are usually referred to as methylidene complexes.[10]

At the dative extreme, the σ^2 lone pair of a singlet methylene overlaps with an empty metal s + d_{z^2} hybrid orbital to form the σ bond. A metal d_{xz} lone pair overlaps with the empty carbon p_x orbital to form the π bond. $(CO)_5WC(Ph)(OCH_3)$ is a typical example of such dative bonding.[11] We refer to metal–methylene complexes of this type as carbene complexes. Metal–carbene and metal–alkylidene complexes show very different chemical reactivity, reflecting the qualitatively different types of metal–carbon bonding.[10,11]

The basic conclusion from numerous calculations on MCH_2^+ species[12,13] is that the bonding is covalent. The present calculations support this bonding picture, as discussed below in section 4.1. Details of the calculations are provided in section 2 and the theoretical results are presented in section 3. Section 4 includes a discussion of the various contributions to the bond energies and a generalization of the present results to related systems such as metal methylidynes MCH^+. Conclusions are summarized in section 5.

2. Calculational Details

2.1. Geometry Optimizations. Since no experimental information is available about the geometries of the MCH_2^+ ions, we examined possible isomers of $TaCH_2^+$ to determine if the M=CH_2 structure is indeed favored. Geometries of singlet H_2TaC^+ (**1**),

* To whom correspondence should be addressed.
† Permanent address: National Institute of Standards and Technology, Chemical Kinetics and Thermodynamics Division, Gaithersburg, Maryland 20899.
‡ Contribution No. 8914.
® Abstract published in *Advance ACS Abstracts*, August 15, 1994.

(1) (a) Martinho Simões, J. A.; Beauchamp, J. L. *Chem. Rev.* **1990**, *90*, 629–688. (b) Collman, J. P.; Garner, J. M.; Hembre, R. T.; Ha, Y. *J. Am. Chem. Soc.* **1992**, *114*, 1292–1301.
(2) Ohanessian, G.; Goddard, W. A., III *Acc. Chem. Res.* **1990**, *23*, 386–392.
(3) Irikura, K. K.; Beauchamp, J. L. *J. Phys. Chem.* **1991**, *95*, 8344–8351.
(4) Irikura, K. K.; Beauchamp, J. L. *J. Am. Chem. Soc.* **1991**, *113*, 2769–2770.
(5) Buckner, S. W.; MacMahon, T. J.; Byrd, G. D.; Freiser, B. S. *Inorg. Chem.* **1989**, *28*, 3511–3518.
(6) Irikura, K. K.; Beauchamp, J. L. *J. Am. Chem. Soc.* **1989**, *111*, 75–85.
(7) (a) Ranasinghe, Y. A.; MacMahon, T. J.; Freiser, B. S. *J. Phys. Chem.* **1991**, *95*, 7721–7726. (b) In one study, it could not be determined that excited Zr^+ was not responsible for $ZrCH_2^+$ formation: Irikura, K. K.; Beauchamp, J. L. Unpublished. (c) $D(Zr^+–CH_2)$ = 101 ± 3 kcal/mol was obtained in ref 8, which makes reaction 1 endothermic by about 10 kcal/mol for Zr^+.
(8) Bauschlicher, C. W., Jr.; Partridge, H.; Sheehy, J. A.; Langhoff, S. R.; Rosi, M. *J. Phys. Chem.* **1992**, *96*, 6969–6973.
(9) Sunderlin. L. S.; Armentrout, P. B. *J. Am. Chem. Soc.* **1989**, *111*, 3845–3855.
(10) Schrock, R. R. *Acc. Chem. Res.* **1979**, *12*, 98–104.
(11) Fischer, E. O. *Adv. Organomet. Chem.* **1976**, *14*, 1–32.
(12) Early calculations: (a) Rappé, A. K.; Goddard, W. A., III *J. Am. Chem. Soc.* **1977**, *99*, 3966–3968. (b) Carter, E. A.; Goddard, W. A., III *J. Am. Chem. Soc.* **1986**, *108*, 2180–2191.
(13) Musaev, D. G.; Morokuma, K.; Koga, N. *J. Chem. Phys.* **1993**, *99*, 7859–7872.

0002-7863/94/1516-8733$04.50/0

Table 1. Optimized Geometries and Relative Energies for Selected States of Metal Methylidene Ions MCH_2^+, Calculated Using the Small Basis Set at the GVB Level Indicated[a]

M	level	nonbonding configuration $1a_1 2a_1 a_2 b_2$	state symmetry	r(M–C) (Å)	r(C–H) (Å)	θ(MCH) (deg)	energy[b] (kcal/mol)
La	GVB(2/4)	0000	$^1A_1$	2.253	1.089	124.1	0.0
	5-ref-CISD[c,d]	0000	$^1A_1$	2.155	1.109	123.9	−1.8[e]
	GVB(1/2)	0000†	$^3A_1$	2.562	1.085	124.3	31.4
Hf	GVB(2/4)	1000	$^2A_1$	1.998	1.087	123.3	0.0
	GVB(2/4)	0010	$^2A_2$	2.018	1.087	123.9	22.3
	GVB(1/2)	1000†	$^4A_1$	2.213	1.084	123.2	33.8
Ta	GVB(2/4)	1010	$^3A_2$	1.951	1.085	122.4	0.0
	GVB(2/4)	1100	$^3A_1$	1.945	1.083	122.3	2.3
	GVB(1/2)	1010†	$^5A_2$	2.174	1.081	121.9	29.7
W	GVB(2/4)	1110	$^4A_2$	1.917	1.085	121.8	0.0
	GVB(1/2)	1111*	$^6A_1$	2.039	1.083	122.9	0.3
	GVB(2/4)	1011	$^4B_1$	1.938	1.082	122.5	5.2
	GVB(1/2)	1110†	$^6A_2$	2.132	1.080	120.7	21.8
Re	GVB(2/4)	1111	$^5B_1$	1.908	1.083	122.0	0.0
	GVB(1/2)	1111†	$^7B_1$	2.124	1.078	120.1	13.9
	GVB(3/6)	1111	$^3B_1$	1.910	1.083	122.1	43.8
Os	GVB(2/4)	1112	$^4A_2$	1.896	1.083	122.4	0.0
	GVB(1/2)	1112†	$^6A_2$	2.102	1.076	119.5	23.0
	GVB(3/6)	0212	$^2A_2$	1.897	1.084	122.4	30.3
	GVB(3/6)	1121	$^2B_2$	1.887	1.082	121.3	33.9
Ir	GVB(2/4)	1212	$^3A_2$	1.868	1.083	121.9	0.0
	GVB(2/4)	1122	$^3A_1$	1.866	1.083	121.9	1.7
	GVB(3/6)	0222	$^1A_1$	1.859	1.083	121.5	18.2
	GVB(1/2)	1212†	$^5A_2$	2.097	1.074	118.1	33.5
Pt	GVB(2/4)	1222	$^2A_1$	1.860	1.082	121.6	0.0
	GVB(1/2)	1222†	$^4A_1$	2.103	1.073	116.7	44.3
Au	GVB(2/4)	2222	$^1A_1$	2.034	1.082	123.3	0.0
	MR-CISD[d]	2222	$^1A_1$	1.889	1.099	122.3	−0.5[d,e]
	GVB(1/2)	2222†	$^3A_1$	2.204	1.073	114.7	69.6

[a] With the molecule in the yz plane and the z-axis along the M–C bond, the metal–carbon double bond uses an a_1 orbital ($s+d_{z^2}$) and a b_1 orbital (d_{xz}) on the metal. This leaves four metal nonbonding orbitals, $1a_1$ ($s-d_{z^2}$), $2a_1$ ($d_{x^2-y^2}$), a_2 (d_{xy}), and b_2 (d_{yz}). One exception, indicated with an asterisk, has only one electron in the π bond. A dagger indicates that the π bond is triplet-coupled instead of singlet-coupled. [b] At the level of theory used in the geometry optimization and relative to the most stable state optimized. [c] CISD using the five reference configurations 2020, 2002, 0202, and 1111 ($\sigma\sigma^*\pi\pi^*$). [d] Using the large basis set; see Calculational Details. [e] Compared with the same calculation using the geometry that is obtained with the smaller basis set and at the GVB(2/4) level.

singlet $HTaCH^+$ (**2**), and triplet $TaCH_2^+$ (**3**) were optimized assuming C_1, C_1, and C_{2v} symmetry, respectively. In order to treat the different isomers in a theoretically consistent way, five, five, and four generalized valence-bond (GVB) pairs were used for **1**, **2**, and **3**, respectively.[14] At the optimized geometries, relative energies were evaluated at the GVB-RCI level. GVB-RCI is a small configuration interaction calculation that includes all excitations within each GVB pair. Thus, with five pairs there are $3^5 = 243$ spatial configurations. The GVB-RCI calculations yield relative energies of 98.9 (**1**), 8.6 (**2**), and 0.0 (**3**) kcal/mol. The

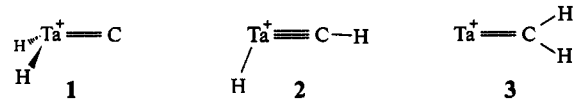

1 **2** **3**

methylidene structure is therefore favored for Ta. All three isomers contain four bonds, but H_2TaC^+ and $HTaCH^+$ are disfavored because metal–hydrogen bonds are no more than two-thirds as strong as carbon–hydrogen bonds.[2] H_2TaC^+ and $HTaCH^+$ also suffer a relatively large loss in exchange energy because of the greater number of bonds to the metal center (see Discussion, section 4, below). The methylidene structure is even more favored for the other metals, which either cannot form four covalent bonds (La^+, Hf^+, Pt^+, Au^+) or have larger exchange energy losses (W^+, Re^+, Os^+, Ir^+).

Metal methylidene ion geometries were determined at the GVB(2/4) level (generalized valence bond, with two electron pairs, each occupying two orbitals) using analytic gradients[15] and assuming C_{2v} symmetry. For alternative low-spin states, we used GVB(3/6) calculations in order to be consistent with the high-spin states.[14] Core electrons on each metal atom were replaced by a relativistic effective potential, so that only the valence and outer core electrons ($5s^25p^6$) were treated explicitly.[16] The corresponding Hay/Wadt metal basis sets were contracted (s331 p311 d21) as previously optimized for the atomic ions.[17] Split-valence (VDZ) basis sets[18] were used on carbon (s721 p41) and hydrogen. The hydrogen basis was contracted (31) and scaled by 1.2. A set of polarization d functions was also included on the carbon ($\alpha = 0.69$).[19] For $LaCH_2^+$ and $AuCH_2^+$, geometries were also determined at the MR-CISD level (multiple-reference configuration interaction including all single and double excitations) using larger basis sets, as described below. These high-level optimizations yield M–C bonds about 0.12 Å shorter and C–H bonds about 0.02 Å longer, but the bond energies differ by less than 2 kcal/mol. Thus, the GVB-level geometries are considered adequate for determining energetics.

Some high-spin states with a metal–carbon bond order less than two were investigated using the smaller basis set. For consistency these were done at the GVB(1/2) level. Although these states have a smaller bond order, they also have greater exchange stabilization and must be considered. The results are included in Table 1.

(14) A balanced calculation provides an equal number of orbitals for an equal number of electrons. For example, a 1-pair calculation of CH_2 ($\tilde{a}\,^1A_1$) should be compared with a 0-pair calculation of CH_2 ($\tilde{X}\,^3B_1$), but 2 pairs must be used for both of the C_2H_4 isomers ethylene and singlet methylcarbene.

(15) Using GVB, a suite of electronic structure programs written at the California Institute of Technology: Goddard, W. A., III; Bair, R. A.; Rappé, A. K.; Bobrowicz, F.; Harding, L. B.; Yaffe, L. Unpublished.

(16) Hay, P. J.; Wadt, W. R. *J. Chem. Phys.* **1985**, *82*, 299–310.
(17) Ohanessian, G.; Brusich, M. J.; Goddard, W. A., III *J. Am. Chem. Soc.* **1990**, *112*, 7179–7189.
(18) Huzinaga, S. *J. Chem. Phys.* **1965**, *42*, 1293.
(19) Carter, E. A.; Goddard, W. A., III *J. Phys. Chem.* **1984**, *88*, 1485–1490.

Table 2. Calculated, Experimental, and Empirically Corrected Bond Energies for Third-Row Transition Metal Methylidene Ions, $D(M^+–CH_2)^a$

metal	calcd D_e (kcal/mol)[b]	expt D_0 (kcal/mol)	corrected D_0 (kcal/mol)[b]	recommended D_0 (kcal/mol)
La	89.8	98 ± 1.5[c]	102 ± 5	98 ± 1.5
Hf	92.0	102 ± 9[d]	104 ± 5	104 ± 5
Ta	102.8	>111[d,e]	115 ± 5	115 ± 5
W	98.9	~111[d]	111 ± 5	111 ± 3
Re	85.1	102 ± 9[d]	97 ± 5	97 ± 4
Os	98.	>111[d,f]	110 ± 6	113 ± 3
Ir	110.9	>111[d]	123 ± 5	123 ± 5
Pt	111.3	>111[d]	123 ± 5	123 ± 5
Au	77.2	>95[g] (> 92.4)[g,h]	89 ± 7	94 ± 2

[a] Bond strengths were calculated at the MR-CISD level using the larger basis set (see Calculational Details). [b] This work. [c] Reference 9. [d] Reference 3. [e] Reference 5. [f] Reference 6. [g] Reference 25. [h] Based on re-interpretation of experimental results (see section 3.1).

2.2 Thermochemistry. A number of reasonable electronic states were considered for each molecule. The ground state configuration and spin were determined from the GVB calculations described above. For molecules with very low-lying excited states, this may lead to an incorrect ground state assignment. Such a mistake would have little effect on the thermochemistry.

Bond energies were obtained at the MR-CISD level using a larger and more flexible basis set. The reference orbitals were generated from a CASSCF(n/n) wave function (self-consistent, complete active space, involving all configurations with n electrons distributed among n orbitals).[20] The number of electrons n was chosen to include all unpaired electrons plus the four involved in the GVB description of the metal–carbon double bond. For example, a CASSCF(5/5) reference was used for both $HfCH_2^+$ and $PtCH_2^+$. All configurations with weights greater than 0.05 were used as reference configurations in the CI.

The basis set was chosen using the calculated bond energy in $LaCH_2^+$ as the figure of merit. The small basis set used for the geometry optimization yields a value of 79.8 kcal/mol. Any fixed contraction of the metal basis set is expected to bias the results toward the particular atomic charge and atomic electron configuration for which the contraction was developed. The metal basis was therefore uncontracted for better flexibility. This increases the bond energy by 4.3 kcal/mol to 84.1 kcal/mol. Replacing the carbon VDZ basis with a triple-split (VTZ) set[21] has little effect, bringing the bond energy to 84.2 kcal/mol. Finally, a set of f functions was added to the metal, with the exponent optimized for the total energy of MCH_2^+ at the Hartree–Fock level. The optimized exponents α(f) are 0.43, 0.46, 0.48, 0.52, 0.57, 0.66, 0.71, 0.78, and 0.82 for the metals from La to Au, respectively. The metal f functions raise the calculated bond energy in $LaCH_2^+$ by 5.9 kcal/mol to 90.1 kcal/mol, which can be compared with the experimental value of 98 ± 1.5 kcal/mol.[9] We feel that this accuracy is sufficient to recover the relative bond energies at reasonable cost.

The bond energies calculated for all MCH_2^+ cases using the large basis set (the polarized, uncontracted metal basis, the polarized, VTZ carbon basis, and the VDZ hydrogen basis) are listed in Table 2. Larger and more accurate bond energies would be obtained by further augmentation of the metal basis, in particular by addition of a second set of polarization functions. This has been demonstrated in recent calculations of the potential energy surface for the reaction between Ir^+ and CH_4.[22]

For $HfCH_2^+$, the high-spin dissociation limit involves Hf^+ in its ^4F excited state. The calculated bond dissociation energy was therefore decreased by the experimental ^4F excitation energy of 13.0 kcal/mol to determine the adiabatic dissociation energy.[23]

In the case of $OsCH_2^+$, the number of open shells and the number of valence electrons combined to exceed the limitations of the CI programs (11 open shells for this number of electrons). For the equilibrium geometry, it is acceptable simply to restrict the number of open shells in the CI, since analogous restrictions on $ReCH_2^+$ and $IrCH_2^+$ raise the energy by only 0.4 and 0.8 kcal/mol, respectively. For the corresponding dissociated geometries, however, this restriction leads to much larger errors of 11.5 and 18.4 kcal/mol, respectively, relative to the unrestricted calculations. Since these errors are quite different, it is not possible to infer the appropriate correction to the $OsCH_2^+$ bond energy of 108.6 kcal/mol from the restricted calculation. As an alternative, the dissociated molecules were investigated in the lower-spin states corresponding to dissociation to singlet CH_2 ($\tilde{a}\ ^1A_1$). The CI programs[20] can accommodate this state of $Os^+\cdots CH_2$ because of the reduced number of open shells. This low-spin dissociated state was calculated to be higher than the corresponding high-spin state by 13.5, 15.0, and 13.4 kcal/mol for $LaCH_2^+$, $ReCH_2^+$, and $IrCH_2^+$, respectively. For $OsCH_2^+$, the calculated bond energy of 112.0 kcal/mol (to singlet CH_2) was therefore corrected by 14 kcal/mol to yield an adiabatic value of 98 kcal/mol.

3. Results

3.1. Bond Strengths. Comparison with the available experimental data in Table 2 indicates that the calculated bond strengths are too low.[24] The disagreement with experiment is worst for $AuCH_2^+$.[25] However, that experimental limit is based upon a minor reaction (6%) of laser-ablated Au^+ with CH_3I. Minor reactions of ions generated by laser ablation at low pressure are generally suspect because some ions are born electronically or translationally hot.[26,27] If this reaction is therefore rejected in favor of the analogous major reaction (70%) between Au^+ and CH_3Br, the implied lower limit for $D(Au^+–CH_2)$ is 92.4 kcal/mol,[25] closer to our calculated value.

The calculated values are too low by 8 ± 1.5 kcal/mol for $LaCH_2^+$, at least 8 kcal/mol for $TaCH_2^+$, 12 ± 3 kcal/mol for WCH_2^+, at least 13 kcal/mol for $OsCH_2^+$, and at least 15 kcal/mol for $AuCH_2^+$. For $IrCH_2^+$, our value is 8 ± 3 kcal/mol lower than recently recommended.[22] Giving more weight to the WCH_2^+ results (in the center of the period), we apply a uniform correction of 12 kcal/mol to our calculated bond energies. Corrections of similar magnitude have been used in other calculations of transition metal ion thermochemistry.[8,28] Since the discrepancies with experiment range from 7 to >15 kcal/mol, we expect our corrected values to be accurate to 5 kcal/mol. A larger uncertainty of 6 kcal/mol for $OsCH_2^+$ is assigned because of the difficulties in the calculations for this molecule (see section 2.2). Since the bonding is rather different in $AuCH_2^+$ than in the other MCH_2^+ (see section 4.1 below), our uniform correction is more questionable for $AuCH_2^+$ and we assign it a larger uncertainty of 7 kcal/

(20) Using MOLECULE-SWEDEN, an electronic structure program suite: Almlöf, J.; Bauschlicher, C. W.; Blomberg, M. R. A.; Chong, D. P.; Heiberg, A.; Langhoff, S. R.; Malmqvist, P.-Å.; Rendell, A. P.; Roos, B. O.; Siegbahn, P. E. M.; Taylor, P. R. Unpublished.

(21) Brusich, M. J.; Goddard, W. A., III Unpublished. Based upon the following: Huzinaga, S.; Sakai, Y. *J. Chem. Phys.* **1969**, *50*, 1371–1381.

(22) Perry, J. K.; Ohanessian, G.; Goddard, W. A., III *Organometallics* **1994**, *13*, 1870–1877.

(23) Moore, C. E. *Atomic Energy Levels*; NSRDS-NBS 35 (reprint of NBS circular 467); U.S. Government Printing Office: Washington, D.C., 1971; Vol. 3.

(24) Reference 13 describes another recent MR-CISD study of $IrCH_2^+$, using a similar basis set, which yielded a bond strength of 113 kcal/mol, in good agreement with our own uncorrected value of 110.9 kcal/mol.

(25) Chowdhury, A. K.; Wilkins, C. L. *J. Am. Chem. Soc.* **1987**, *109*, 5336–5343.

(26) (a) Kang, H.; Beauchamp, J. L. *J. Phys. Chem.* **1985**, *89*, 3364–3367. (b) Wiedeman, L.; Helvajian, H. *J. Appl. Phys.* **1991**, *70*, 4513–4523. (c) Haglund, R. F., Jr.; Affatigato, M.; Arps, J. H.; Tang, K.; Niehof, A.; Heiland, W. *Nucl. Instrum. Meth. B* **1992**, *65*, 206–211.

(27) Elnakat, J. H.; Dance, I. G.; Fisher, K. J.; Willett, G. D. *Polyhedron* **1993**, *12*, 2477–2487.

(28) Bauschlicher, C. W., Jr.; Langhoff, S. R.; Partridge, H. *J. Phys. Chem.* **1991**, *95*, 6191–6194.

Table 3. Vertical Relative Energies for Metal Methylidene Ions MCH_2^+ at Partially Optimized Geometries[a]

metal	level	non-bonding[b] config $1a_1 2a_1 a_2 b_2$	state symm	geometry used r(MC)/r(CH)/θ(MCH) (Å/Å/deg)	energy[c] (kcal/mol)
Hf	GVB(2/4)	1000	$^2A_1$	2.014/1.089/123.4	0.0
	GVB(2/4)	0010	$^2A_2$		22.2
	GVB(2/4)	0001	$^2B_2$		34.6
Ta	GVB(2/4)	1010	$^3A_2$	1.925/1.092/121.6	0.0
	GVB(2/4)	1100	$^3A_1$		2.2
	GVB(2/4)	1001	$^3B_2$		22.0
	GVB(2/4)	0011	$^3B_1$		27.8
W	GVB(2/4)	1110	$^4A_2$	1.925/1.092/121.6	0.0
	GVB(2/4)	1011	$^4B_1$		5.3
	GVB(2/4)	1101	$^4B_2$		6.1
Os	GVB(2/4)	1112	$^4A_2$	1.938/1.082/122.5	0.0
	GVB(2/4)	1121	$^4B_2$		5.4
	GVB(2/4)	1211	$^4B_1$		5.6
	GVB(1/2)	1112	$^6A_2$		28.9
	GVB(3/6)	0212	$^2A_2$		30.2
	GVB(3/6)	1121	$^2B_2$		34.2
Ir	GVB(2/4)	1212	$^3A_2$	1.90/1.09/122	0.0
	GVB(2/4)	1122	$^3A_1$		1.7
	GVB(2/4)	2121	$^3B_2$		18.3
	GVB(3/6)	0222	$^1A_1$		18.5
	GVB(2/4)	2211	$^3B_1$		18.8
Pt	GVB(2/4)	1222	$^2A_1$	1.860/1.082/121.6	0.0
	GVB(2/4)	2212	$^2A_2$		11.7
	GVB(2/4)	2221	$^2B_2$		24.2

[a] The small basis set was used at the GVB level indicated. [b] See Table 1. [c] At the level of theory indicated and relative to the most stable state listed in this table.

mol. In support of our corrected bond energies, we note that (1) they parallel the experimental rate measurements and (2) the resulting intrinsic bond energies (see Discussion) are the same for the late metals. The corrected values are listed in Table 2.

Combining our corrected bond energies with the experimental constraints leads to the recommended values listed at the extreme right in Table 2. Throughout the Discussion below, we use these recommended values. Note that the uncertainties assigned to the recommended values are derived from the overlap between the (corrected) theoretical and the experimental ranges (Table 2). Thus, the recommended values are simply the experimental values for $LaCH_2^+$ and WCH_2^+, and the reduced uncertainties for $ReCH_2^+$, $OsCH_2^+$, and $AuCH_2^+$ reflect the narrow ranges of values that are consistent with both theoretical and experimental results.

3.2. Geometries and Electronic States. Results of geometry optimizations for selected electronic states of the metal methylidene ions are summarized in Table 1. Additional electronic states were also evaluated, but without geometry optimization. The corresponding vertical excitation energies are collected in Table 3. Although these energies are not at optimum geometries, comparison with values in Table 1 reveals that the energy differences are not sensitive to small differences in geometry. The relative state energies listed in Tables 1 and 3 were calculated at the GVB level. For $IrCH_2^+$, state energies calculated at the higher MR-CISD level[13] are in fair agreement with our GVB results.

As a further test of the counterplay between bonding and exchange energy (see Discussion), a few high-spin states were investigated for WCH_2^+ and $ReCH_2^+$, which have the most unpaired electrons. For WCH_2^+, the $^6A_1$ state, at the appropriate GVB(1/2) level, is placed only 0.3 kcal/mol above the ground $^4A_2$ state. Although close, it is probably not the ground state, since better treatment of electron correlation is expected to increase the gap.

4. Discussion

4.1. Orbital Description. Despite the non-monotonic changes in M^+–CH_2 bond energies across the third transition row (see Table 2 and Figure 1), the variations can be explained simply in terms of promotion energy and exchange energy. These concepts are used widely in comparisons of low-spin and high-spin coordination compounds,[29] and their importance in metal ion chemistry has been established both theoretically[2,8,30] and experimentally.[31] For the molecules at hand, promotion to a $d^{n-1}s^1$ configuration has been correlated with the rate of reaction 1.[3] The corresponding promotion energies to high-spin $d^{n-1}s^1$ configurations are listed in Table 4. J-averaged energies (under L–S coupling) are listed for compatibility with the present nonrelativistic calculations. As for the first- and second-row transition metal methylidene ions[8] and the diatomic transition metal hydride cations,[17,32,33] describing the energetics in terms of a $d^{n-1}s^1$ configuration is sucessful despite significant contributions from the d^n configuration. Population percentages relevant to the bonding and hybridization are illustrated in Figures 2 and 3.

Net atomic charges and metal d-orbital populations are listed in Table 5. The clearest trend in Table 5 is probably the monotonic decrease in charge separation as one progresses from $LaCH_2^+$ ($La^{+1.30}$) to $AuCH_2^+$ ($Au^{+0.71}$). This reflects the greater electronegativity of the later transition metals and is also evident for second- and third-row MH^+ and for first- and second-row MCH_2^+.[8,17,33] From Figure 2, it is apparent that the change in charge balance occurs in the π bond. This is clearly illustrated in the pair orbital plots of Figure 4. In contrast, the σ bond remains covalent across the row (Figures 2 and 5). For gold, the

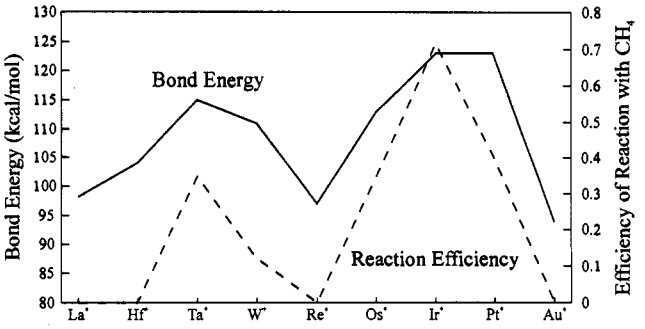

Figure 1. Corrected values of $D(M^+–CH_2)$ and experimental rates (from ref 3) for reaction 1.

Table 4. Promotion Energies, Detailed Exchange Energies, Net Exchange Energies, and Intrinsic Bond Energies for Doubly-Bonded MCH_2^+ (in kcal/mol)

metal	promotion energy[a]	av K_{sd}[b]	av K_{dd}[b]	net exchange[c]	intrinsic bond energy
La	5.4	9.4		4.7	108
Hf	10.4	12.7	10.5	17.9	132
Ta	0	12.5	11.6	30.3	145
W	0	12.4	12.6	43.6	155
Re	0	11.9	13.5	56.7	154
Os	0	12.0	14.1	45.2	158
Ir	0[d]	11.7	14.9	32.5	156
Pt	13.7	11.5	15.8	19.4	156
Au	43.0	11.4		5.7	143

[a] To the most stable high-spin $d^{n-1}s^1$ configuration. Unless noted, calculated from data in ref 23. [b] Average over all high-spin $d^{n-1}s^1$ configurations. [c] Exchange energy lost by high-spin $d^{n-1}s^1$ metal ion upon forming two covalent bonds using one s and one d orbital. [d] van Kleef, Th. A. M.; Metsch, B. C. *Physica C* **1978**, *95*, 251–265.

(29) For example: Cotton, F. A.; Wilkinson, G. *Advanced Inorganic Chemistry*, 4th ed.; John Wiley & Sons: New York, 1980; pp 644 ff.
(30) Carter, E. A.; Goddard, W. A., III *J. Phys. Chem.* **1988**, *92*, 5679–5683.
(31) Armentrout, P. B.; Sunderlin, L. S.; Fisher, E. R. *Inorg. Chem.* **1989**, *28*, 4436–4437.
(32) Schilling, J. B.; Goddard, W. A., III; Beauchamp, J. L. *J. Am. Chem. Soc.* **1986**, *108*, 582–584.
(33) Schilling, J. B.; Goddard, W. A., III; Beauchamp, J. L. *J. Am. Chem. Soc.* **1987**, *109*, 5565–5573.

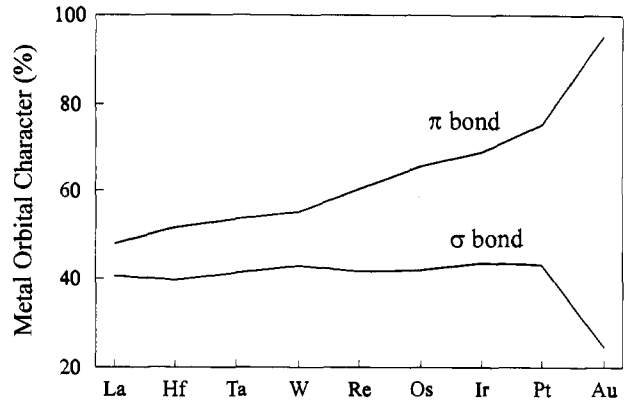

Figure 2. Contribution of metal-centered orbitals to the metal–carbon bonds of MCH_2^+, based upon mulliken populations from GVB(2/4) wave functions.

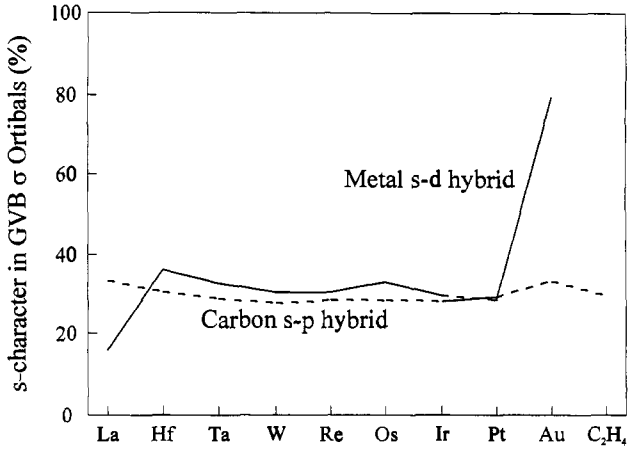

Figure 3. Metal s–d and carbon s–p hybridizations in the σ bonds of MCH_2^+ and of ethylene. Hybridizations are expressed as % s character and are based upon Mulliken populations from GVB(2/4) wave functions.

Table 5. Valence Mulliken Populations from GVB(2/4) Wave Functions

molecule	metal s	metal d	carbon s	carbon p	metal charge	carbon charge
$LaCH_2^+$ ($^1A_1$)	0.11	1.59	1.47	3.30	1.30	–0.80
$HfCH_2^+$ ($^2A_1$)	0.84	1.85	1.48	3.32	1.24	–0.82
$TaCH_2^+$ ($^3A_2$)	0.80	2.98	1.49	3.28	1.18	–0.80
WCH_2^+ ($^4A_2$)	0.79	4.07	1.50	3.24	1.13	–0.76
$ReCH_2^+$ ($^5B_1$)	0.72	5.17	1.51	3.13	1.09	–0.68
$OsCH_2^+$ ($^4A_2$)	0.70	6.25	1.51	3.01	1.00	–0.57
$IrCH_2^+$ ($^3A_2$)	0.67	7.37	1.51	2.94	0.92	–0.51
$PtCH_2^+$ ($^2A_1$)	0.61	8.53	1.54	2.86	0.84	–0.45
$AuCH_2^+$ ($^1A_1$)	0.53	9.72	1.63	2.67	0.71	–0.34
C_2H_4			1.29	3.07		–0.41
WCH_2^+ ($^6A_1$)[a]	0.74	4.17	1.56	3.03	1.03	–0.63
$ReCH_2^+$ ($^7B_1$)[a]	0.76	5.01	1.51	3.22	1.16	–0.76

[a] GVB(1/2) calculation.

metal–carbon bonding is close to the purely dative case of Scheme 1 (Figure 2). For lanthanum, there is relatively little metal s-character in the σ bond; the hybridization is approximately sd^5, rather than sd^2 as for the other metals (Figure 3). The bonding is similar among the other metals (Hf, Ta, W, Re, Os, Ir, and Pt), except for the increasing π back-donation.

4.2. Exchange Energies. Exchange energies K_{sd} and K_{dd} were also calculated for the $d^{n-1}s^1$ atomic ions and are included in Table 4. The K_{dd} values represent averages over all high-spin d-orbital occupations. K_{sd} increases abruptly from La^+ to Hf^+ because of the lanthanide contraction, which shrinks the 6s orbital so that its radial extent more closely matches that of the 5d orbitals. Likewise, the increase in K_{dd} across the period reflects the decreasing size of the 5d orbitals, which brings the d-electrons closer together. Exchange energy is lost upon covalent bond formation; the associated bookkeeping has been discussed

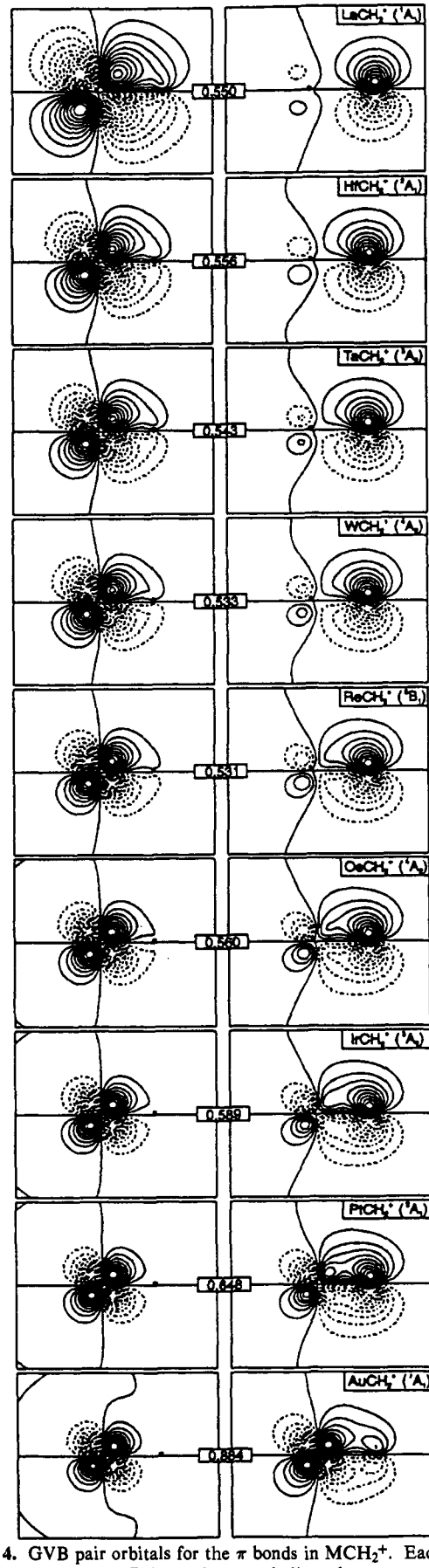

Figure 4. GVB pair orbitals for the π bonds in MCH_2^+. Each orbital contains one electron. Pair overlaps are indicated.

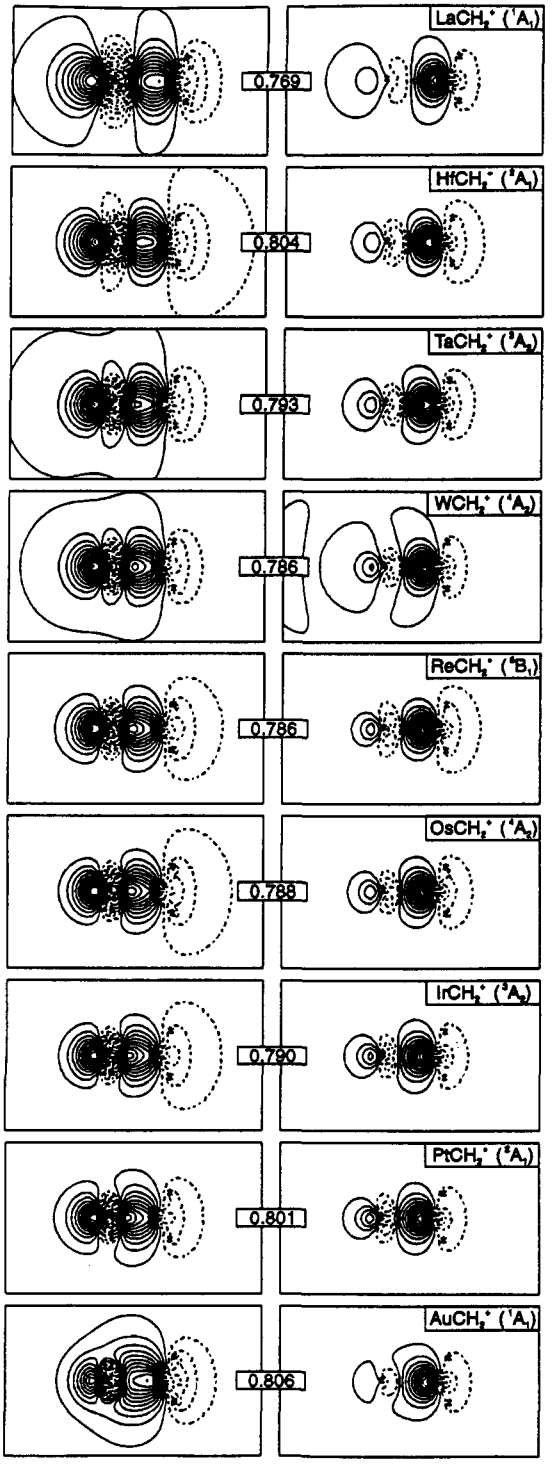

Figure 5. GVB pair orbitals for the σ bonds in MCH_2^+. Each orbital contains one electron. Pair overlaps are indicated.

elsewhere[34] and is illustrated in Scheme 2. The electron configuration for the bare metal ion is indicated on the left. The orbitals that are spin-paired with CH_2 are indicated on the right. Assuming that the bonding is purely covalent, each spin-paired orbital on the metal is up spin (α) half the time and down spin (β) half the time. This leads to the MCH_2^+ exchange energies indicated on the right side of Scheme 2. The amount of exchange energy lost by the $d^{n-1}s^1$ metal ion upon bonding to CH_2 rises and then falls across the row.[30] For example, Hf^+ and Pt^+ lose $K_{sd} + {}^1/_2K_{dd}$, while Re^+ loses ${}^5/_2K_{sd} + 2K_{dd}$. The net amounts of exchange energy lost are listed in Table 4, where it is assumed that the s-orbital and one d-orbital are employed in bonding.

4.3. The Intrinsic Bond Strength. Adjusting the bond strengths

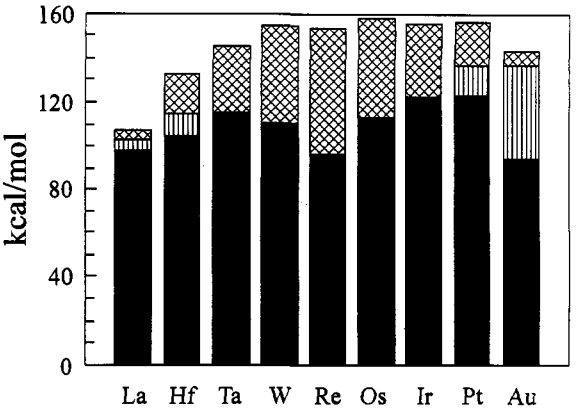

Figure 6. Contributions to the bond energies in MCH_2^+. Solid fill shows the recommended bond strengths, vertical fill shows the promotion energies, and crossed fill shows the exchange energies. The combined height represents the intrinsic bond energy (eq 2).

Scheme 2

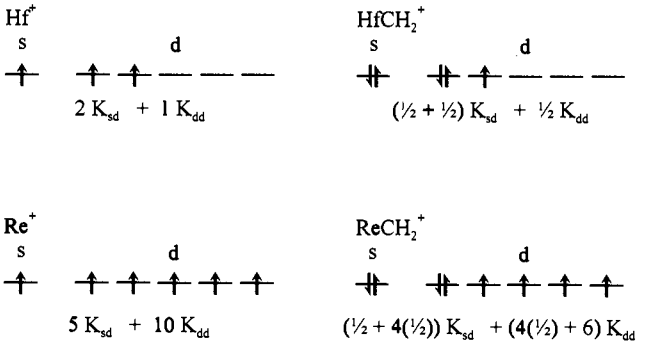

D_0^{actual} for promotion and exchange energies leads to the "intrinsic" $M^+{=}{=}CH_2$ bond energies $D_0^{intrinsic}$ (eq 2).[34] We have used

$$D_0^{actual} = D_0^{intrinsic} - \Delta E_{promotion} - \Delta E_{exchange} \qquad (2)$$

our recommended bond energies (Table 2) as D_0^{actual} in order to calculate the $D_0^{intrinsic}$ values listed in Table 4. For the late metals W to Pt, the intrinsic bond energy is remarkably constant at about 155 kcal/mol, suggesting that the concept of intrinsic bond energies can be useful for predicting bond strengths in methylidene complexes of these metals.[30] Figure 6 illustrates the decomposition of the bond energies into the intrinsic bond strength, exchange energy, and promotion energy.

4.4. Comparison with Experiment. The rate at which M^+ reacts with methane has been observed to correlate with the promotion and exchange energy lost by the metal ion upon bonding to a methylene ligand.[3] There is a corresponding relationship between methane reaction rates and the metal–methylidene bond strengths. This correlation, illustrated in Figure 1, indicates that the barrier for reaction 1 is small or zero. Such thermodynamic control is fairly common for ion–molecule reactions, in which the electrostatic attraction between the ion and the polarizable neutral reaction partner provides a substantial amount of energy to the ion–molecule complex.[35]

For Pt^+, the observed rate of reaction 1 is somewhat less than would be expected from the Pt^+–CH_2 bond energy (Figure 1). This suggests that the potential energy surface for $Pt^+ + CH_4$ contains a small barrier that is not present on the other $M^+ + CH_4$ surfaces.[22]

(34) Goddard, W. A., III; Harding, L. B. *Annu. Rev. Phys. Chem.* **1978**, *29*, 363–396.

(35) Talrose, V. L.; Vinogradov, P. S.; Larin, I. K. In *Gas Phase Ion Chemistry*; Bowers, M. T., Ed.; Academic: New York, 1979; Vol. 1, Chapter 8.

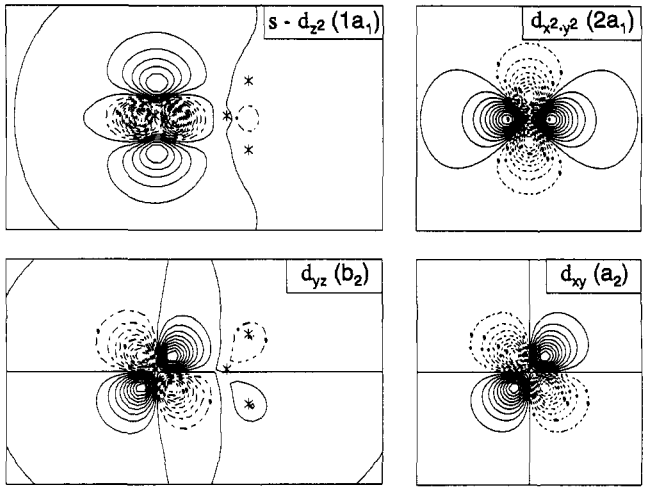

Figure 7. The singly-occupied, nonbonding d orbitals in $ReCH_2^+$ ($^5B_1$).

Table 6. Ground State Symmetry and Occupation of Nonbonding Orbitals for MCH_2^+ [a]

metal	$1a_1\ a_2\ 2a_1\ b_2$	symmetry
La	0 0 0 0	$^1A_1$
Hf	1 0 0 0	$^2A_1$
Ta	1 1 0 0	$^3A_2$
W	1 1 1 0	$^4A_2$
Re	1 1 1 1	$^5B_1$
Os	1 1 1 2	$^4A_2$
Ir	1 1 2 2	$^3A_2$
Pt	1 2 2 2	$^2A_1$
Au	2 2 2 2	$^1A_1$

[a] The $1a_1$ orbital is largely ($s–d_{z^2}$), while the $2a_1$ orbital is mostly $d_{x^2-y^2}$.

4.5. Ground State Symmetries. In addition to the bonding orbitals described in Scheme 1, the valence electrons may occupy four nonbonding orbitals on the metal: $s–d_{z^2}$ ($1a_1$), $d_{x^2-y^2}$ ($2a_1$), d_{xy} (a_2), and d_{yz}(b_2). These orbitals are plotted in Figure 7 for $ReCH_2^+$ ($^5B_1$), in which each nonbonding orbital is singly occupied. The occupation of the nonbonding orbitals for all the MCH_2^+ ground states is summarized in Table 6. Since these orbitals are nearly degenerate, the nonbonding electrons are high-spin coupled in all cases. The first four nonbonding electrons ($HfCH_2^+$ through $ReCH_2^+$) fill orbitals in the order $1a_1$, a_2, $2a_1$, b_2. Interestingly, the last four nonbonding electrons ($OsCH_2^+$ through $AuCH_2^+$), fill in the reverse order (b_2, $2a_1$, a_2, $1a_1$), leading to the electron-hole symmetry apparent in Table 6. This electron-hole symmetry extends to the low-lying excited states. For example, both WCH_2^+ (1110 occupation) and $OsCH_2^+$ (1112 occupation) have $^4B_1$ and $^4B_2$ states lying about 5.5 kcal/mol above the ground state.

4.6. High-Spin States. As discussed above, the metal ion loses substantial exchange energy upon forming two covalent bonds to a CH_2 moiety. Less exchange energy is lost if only a σ bond is formed. For example, starting with the ground state of $ReCH_2^+$ ($^5B_1$) and triplet-coupling the π bond generates the $^7B_1$ state and leads to an exchange stabilization of $2K_{dd}$ (about –27.0 kcal/mol). Of course the π bond is broken, and the net excitation energy is +13.9 kcal/mol (Table 1). Triplet-coupling the orbitals of the π bond in WCH_2^+ ($^4A_2$) generates the $^6A_2$ state with an extra exchange stabilization of $^3/_2K_{dd}$, or –18.9 kcal/mol. This leads to a net excitation energy of +21.8 kcal/mol (Table 1). These two examples suggest that the intrinsic π bond strengths are 40.9 and 40.7 kcal/mol in $ReCH_2^+$ and WCH_2^+, respectively. Starting with the WCH_2^+ ($^6A_2$) excited state and moving the metal π electron into the b_2 nonbonding orbital generates the $^6A_1$ state, which lies 21.5 kcal/mol below the $^6A_2$ state. This is consistent with the π bond order of $^1/_2$ for WCH_2^+ ($^6A_1$). The near-degeneracy of the $^6A_1$ state (bond order = $^3/_2$) with the ground state (bond order = 2) emphasizes the importance of exchange energy in the electronic structure of these metal complexes.

Table 7. Intrinsic π Bond Energies in MCH_2^+, both in kcal/mol and as a Percentage of the Corresponding Total Intrinsic Bond Energies

	intrinsic π bond energy	
metal	kcal/mol	as a % of the total
La	31.4	29
Hf	39.6	30
Ta	41.3	28
W	40.7	26
Re	40.9	27
Os	44.2	28
Ir	48.4	31
Pt	52.2	33
Au	69.6	49

Table 8. Estimated Metal–Carbon Bond Dissociation Energies (kcal/mol) in MCH^+, M = La to Au, Based upon the Intrinsic Bond Energy Model

metal	intrinsic BDE	promotion + exchange	estimated BDE	exp
La	124	10	114	117 ± 8[a]
Hf	172	28	144	
Ta	187	36	151	
W	195	56	139	
Re	195	77	118	
Os	202	59	143	
Ir	204	40	164	
Pt	208	33	175	
Au	143	49	94	

[a] Revised value from ref 36 (see text, section 4.7).

The intrinsic π bond strengths for the different metal complexes are collected in Table 7. Except for gold, the π bond represents a fairly constant fraction (about 29%) of the total intrinsic double bond strength. The π bond of ground state $AuCH_2^+$ is much like a gold d_π lone pair (Figures 2 and 4). Triplet-coupling the π electrons, however, forces one electron onto the carbon. Thus, the large intrinsic π bond energy for $AuCH_2^+$ is a result of the unfavorable electron transfer that results from breaking the π bond.

4.7. Generalization to Other Systems: MCH^+. In order to illustrate how the GVB ideas for MCH_2^+ can be applied to other systems, consider the metal–methylidyne complexes MCH^+. As we found for $HTaCH^+$ (see section 2.1), we expect a methyne (CH) ligand to form a covalent triple bond with M^+, using $s+d_{z^2}$, d_{xz}, and d_{yz} metal orbitals. Assuming that the s orbital and two d orbitals are used to make three covalent bonds, it is straightforward to calculate the exchange energy lost upon bonding.[30] The exchange energies lost upon forming MCH^+ are summarized in Table 8. As for MCH_2^+, the exchange energy rises to a peak at Re, leading us to predict that the metal–carbon bond energies in MCH^+ will have the same double-humped pattern, with a minimum at Re, as found for the MCH_2^+. The intrinsic triple-bond strength is therefore estimated to exceed $D_0^{intrinsic}(M^+ - CH_2)$ by the intrinsic π bond strength (Table 7), with the two exceptions $LaCH^+$ and $AuCH^+$. In $LaCH^+$, the second π bond contains only one electron (total bond order = 2.5), so we augment the intrinsic double bond strength by only half the intrinsic π bond strength. Au^+ can form only a double bond with a CH fragment, so the intrinsic double bond strength is used. Subtracting the promotion and exchange energies from the estimated intrinsic bond strengths leads us to the estimates for $D(M^+–CH)$ listed in Table 8. The only available experimental value is $D(La^+–CH) = 125 \pm 8$ kcal/mol.[36] This experimental value is referenced

(36) Hettich, R. L.; Freiser, B. S. *J. Am. Chem. Soc.* **1987**, *109*, 3543–3548.

to a value of 106 kcal/mol for $D(La^+–CH_2)$, which is too high by 8 kcal/mol.[9] Hence the revised experimental value is $D(La^+–CH) = 117 \pm 8$ kcal/mol, in good agreement with the value of 114 kcal/mol predicted using the intrinsic bond energy method.

5. Conclusions

The simple valence bond model derived from the GVB wave function is consistent with the results of extensive CI calculations and with experiment. This model should be useful in predicting electronic ground states and relative bond energies for other reactive intermediates such as the metal carbynes MCH^+.

Acknowledgment. We thank Jason Perry for many helpful discussions and for modifications to the SWEDEN programs.[20] Support from NSF (CHE 91-00284) is gratefully acknowledged. The facilities of the MSC are supported by grants from NSF-GCAG (ASC-9219368), DOE-AICD, Allied-Signal, Asahi Chemical, Asahi Glass, BP Chemical, Chevron Petroleum Technology Co., BF Goodrich, Vestar, and Xerox.